Available online at www.sciencedirect.com
SCIENCE DIRECT®
Journal of Colloid and Interface Science 274 (2004) 107–117
JOURNAL OF Colloid and Interface Science
www.elsevier.com/locate/jcis

The effect of ultrasound on the particle size and structural disorder of a well-ordered kaolinite

F. Franco,[a,*] L.A. Pérez-Maqueda,[b] and J.L. Pérez-Rodríguez [b]

[a] *Departamento de Química Inorgánica, Cristalografía y Mineralogía, Facultad de Ciencias, Campus de Teatinos, Universidad de Málaga, 29071 Málaga, Spain*

[b] *Instituto de Ciencia de Materiales de Sevilla, Centro Mixto C.S.I.C.-Universidad de Sevilla, C/Américo Vespucio s/n, Isla de la Cartuja, 41092 Seville, Spain*

Received 12 August 2003; accepted 2 December 2003

Abstract

The present study examined the effect of sonication on the particle size and structure of a well-crystallized (KGa-1) kaolinite from Georgia. Sonication produced an important delamination effect as well as a reduction of the other particle-size dimensions. The experiments, carried out under different experimental conditions, showed that particle-size reduction can be controlled through different variables such as power of ultrasonic processor, amount of sample (kaolinite + water), and time of treatment. As a consequence of this particle-size reduction the surface area increases sharply with the sonication time from 8.5 to 83 m^2/g after 20 h with the most energetic treatment. Contrary to what is observed in the grinding treatment, sonication did not cause the amorphization of kaolinite, as observed by XRD and FTIR data. Nevertheless, ultrasound treatment increased the structural disorder, which consisted in increases in the proportion of specific translations $(-a/3 + b/3)$ between adjacent layers in the first hours of treatment, followed by increases in the proportion of random translations between layers.

Keywords: Kaolinite; Sonication; Particle-size reduction; Structural disorder

1. Introduction

Kaolinite [$Al_2Si_2O_5(OH)_4$] is an important industrial raw material having widespread applications, e.g., in ceramics, in the manufacture of paper (as a coating pigment and filler), and in inks and paints (as an extender), as well as an additive in the production of rubber and polymers [1–3]. Parameters such as surface area, brightness, crystallinity, and particle size appear to be important factors controlling the technical applicability of kaolinite [2,4–6].

In the past few years, new applications of kaolinite have been being developed. These applications are mainly related to the sorption properties of kaolinite, very important in retention of radionuclides and heavy metals. In fact, kaolinite is a common accessory mineral in the host rock of radioactive waste deposal [7]. Moreover, Osmanlioglu [8] showed that the inclusion of kaolinite in cement for use in cementation of radioactive waste significantly reduces the leaching rates of the radionuclides. Nevertheless, the sorption capacity of kaolinite is limited because this mineral commonly exhibit a small surface area.

The search for a treatment for increasing the specific surface area (ssa) of kaolinite has been the subject of great interest in the past few years. This surface reactivity can be enhanced with particle-size reduction which, traditionally, has been produced by grinding (either wet or dry) [9–11]. These treatments increase the specific surface area of kaolinite but, at the same time, they produce undesirable effects, such as the degradation of the crystal structure [11,12]. The kinetics of these solid-state mechanochemical modifications depends on a large number of experimental conditions of grinding, such as ratio of weight of samples to weight of balls, number of balls, ball radius, and mill geometry. Several studies have been devoted to the study of the influence of grinding under different experimental conditions on the physicochemical properties of kaolinite. Thus, it has been reported that dry ball milling [11] increases the specific surface area of kaolinite with the grinding time (from 10.20 to 17.73 m^2/g after 15 min of treatment under the experimental conditions reported in [11]). This variation was associ-

* Corresponding author.
E-mail address: ffranco@uma.es (F. Franco).

0021-9797/$ – see front matter
doi:10.1016/j.jcis.2003.12.003

ated with the particle-size reduction. Nevertheless, after prolonged grinding, the particles agglomerate and the surface area decreases after 20 min of grinding, as a consequence of the enhanced surface energy of the ground particles. Baudet et al. [10] showed that using attrition milling provides predominant delamination within the first minutes and a more marked transverse breakage of kaolinite flakes in prolonged treatment. Suraj et al. [9] found that grinding of kaolinite in an oscillatory mill produces almost complete amorphization of the kaolinite structure within 1 h of sonication.

The grinding of kaolinite also causes its partial delamination. According to Farmer and Russell [13], delamination can be examined by IR spectroscopy from the intensity and position of the vibration of the Si–O band which gives a dipole oscillation perpendicular to the plates. For delaminated kaolinite, an infrared absorption occurs when the radiation is perpendicular to the crystal plates. Yariv [14,15] observed, for kaolinite diluted by several alkali chlorides and bromides, that Si–O in-plane vibration (at 1010 cm^{-1}) disappears, indicating that kaolinite is completely transformed into an amorphous material after 120 min of grinding. The persistence of another Si–O in-plane vibration band at 1035 cm^{-1} indicates that the amount of total silica was constant. The dilution with the alkali halide salt delays the amorphization of the clay.

A feasible technique for particle-size reduction is ultrasound. The extended application of ultrasound as a tool for material chemistry began only in 1980. Cavitational collapse sonication in solids leads to microjet and shock-wave impacts on the surface, together with interparticle collisions, which can result in particle-size reduction [16]. Velho and Gomes [17] studied the delamination of diverse Portuguese kaolins through the intercalation of hydrazine hydrate and mechanical methods such as the application of ultrasound in two stages of 5 min. These authors observed that the delamination treatments carried out provide increases of the specific surface area (about 20% of the initial values) and an effective increase in kaolin whiteness. On the other hand, Pérez-Maqueda et al. [18] and Pérez-Rodríguez et al. [19] showed that sonication of macroscopic vermiculite flakes yields submicrometer plate-like particles and that, even after 100 h sonication time, vermiculite was not amorphicized and the crystalline structure was not damaged.

The effect of sonication on kaolinite could be a matter of great interest. In the present study the effect of ultrasound on a well-ordered kaolinite is extensively studied. Changes in particle size, specific surface area, crystallite size, and structure have been analyzed.

2. Experimental details

2.1. Material

The sample used for this study was a low-defect ("well-crystallized") kaolinite from Washington County, Georgia (KGa-1 from the Source Clay Mineral Repository, University of Missouri) with a Hinckley index [20] of 1.19. Before sonication treatment, the original kaolinite (KGa-1) sample consists of pseudohexagonal crystals of 0.5–2 μm and stacks of plates of greater size (Fig. 1).

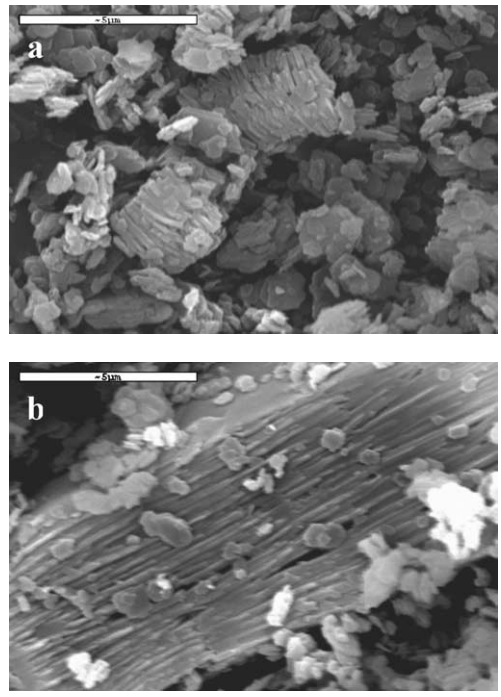

Fig. 1. Scanning electron micrographs of untreated kaolinite.

2.2. Sonication

Different amounts of mixed kaolinite plus freshly deionized water (1.5 g of kaolinite + 40 ml of water and 3 g of kaolinite + 80 ml of water) were subjected to continuous ultrasound treatment for periods ranging from 10 to 75 h in two different high-intensity ultrasonic horns. The ultrasonic treatments were performed using two different Misonic ultrasonic liquid processors of output 750 and 600 W, respectively, both with a 20-kHz converter and tapped titanium disruptor horn of 12.7 mm in diameter that produces a double (peak-to-peak) amplitude of the radiating face of the tip of 120 μm. The horn tip was dipped into a cylindrical jacketed cooling cell 5 cm in internal diameter, where the kaolinite sample was mixed with freshly deionized water. The temperature of the reactor was kept constant at 20 °C during the entire treatment by means of a cooling recirculator. Then treated samples were lyophilized to eliminate the water of the suspension.

Various treatments with different experimental conditions were carried out to evaluate the influence of different parameters such as time of treatment, amount of sample and power of the ultrasonic processor:

Treatment I: 1.5 g of kaolinite + 40 ml of water in a 750-W ultrasonic processor.

Treatment II: 1.5 g of kaolinite + 40 ml of water in a 600-W ultrasonic processor.
Treatment III: 3 g of kaolinite + 80 ml of water in a 600-W ultrasonic processor.

The influence of the amount of sample is evaluated with treatments II and III. In treatment III the amount of sample is larger than in treatment II. Nevertheless, the mass of kaolinite and water was maintained in the same proportion to avoid the influence of changes in the viscosity of the suspensions.

2.3. Sample characterization

A laser method, low-angle laser light scattering (LALLS), was used for the particle size analysis. LALLS (Mastersizer Model, Malvern) is based on the fact that when a particle passes through a laser beam it causes light to be scattered at an angle that is inversely proportional to its size. The procedure consist of capturing the scattering pattern from the dispersion of the sample and of analyzing the pattern using the Mie theory. The measurements were performed on very diluted dispersions at 20 °C. Identical conditions were used for all samples studied here.

Brunauer–Emmet–Teller (BET) specific surface areas (SSA) were obtained with an automatic system (Model 2200 A, Micromeritics Instrument Co., Norcross, GA), using nitrogen gas as an adsorbate at liquid nitrogen temperature. The samples previously were outgassed at 140 °C for 2 h. The equivalent spherical diameter (ESD) was calculated from the SSA by means of the expression

$$\mathrm{ESD} = \left[6/(\sigma S)\right] \times 1000,$$

where ESD is the equivalent spherical diameter (nm), σ is the density of the material (2.64 g cm^{-3}), and S is the SSA (m^2 g^{-1}) determined by BET.

X-ray diffraction patterns were obtained using a Siemens D-5000 diffractometer. The XRD patterns were obtained using Cu$K\alpha$ radiation at 40 kV and 35 mA and a step size of 0.02° 2θ at a counting time of 3 s. Measurements were performed on randomly oriented powder preparations. Defects in kaolinite were characterized using the Hinckley index (*HI*) [20] and the R_2 index of Liètard [21,22]. The HI value was calculated as the ratio of sum of the height above background of the $1\,\bar{1}\,0$ and $1\,1\,\bar{1}$ reflections against the band of overlapping reflections occurring between 20° and 23° 2θ compared to the total height of the $1\,\bar{1}\,0$ above the background. The R_2 index was calculated with the $1\,\bar{3}\,1$ and $1\,3\,1$ reflection intensities and the counts in the valley between them. The apparent coherent scattering thickness of the kaolinite crystals was calculated along the c^* axis, using the $0\,0\,2$ reflection (CS_{002}), and along the b axis, using the $0\,6\,0$ reflection (CS_{060}), according to the Scherrer formula [23].

FTIR spectra were recorded in KBr pellets (2 wt% sample) using a Nicolet spectrometer (20SXB) with a DTGS detector, in the range 40,000–400 cm^{-1}. Resolution was 2 cm^{-1}. Three hundred scans were accumulated to improve the signal-to-noise ratio in the spectra. To avoid grinding effects in the preparation of the disk, samples and KBr were gently mixed manually. The intensity of the Si–O bands was used to normalize the FTIR spectra.

The samples were also studied by scanning electron microscopy (SEM) using a Jeol JSM-5400 model and by transmission electron microscopy (TEM) using a Philips CM 200 model.

3. Results and discussion

3.1. Particle size and specific surface area analysis

Fig. 2 shows the particle-size distribution vs the percentage of particle volume of the untreated kaolinite and after increasing sonication times and different sonication treatments (treatments I, II, III), as estimated by LALLS measurements. The particle distribution of untreated kaolinite (Fig. 2Ia) shows the presence of three populations of particles between 0.1 and 30 μm, with maxima at 0.5, ∼1.8, and ∼9.9 μm.

Treatment I: Under the experimental conditions of treatment I, a sonication period of 10 h causes complete loss of the particles larger than 5 μm. Thus, the distribution curve (Fig. 2Ib) shows the presence of two maxima at 0.43 and ∼1.4 μm. For this time of treatment, the proportion of the smallest particles increases and the maximum of this population shifts from 0.50 to 0.43 μm, whereas the proportion of the 1.8-μm particles, observed in the distribution curve of untreated kaolinite, decreases and the maximum shifts to ∼1.4 μm. On the other hand, after a sonication period of 20 h, the 0.43-μm maximum decreases and shifts to 0.36 μm and the proportion of the 1.4-μm particles strongly decreases. Simultaneously, this distribution curve shows the presence of two other populations of particles with maximum volume percentages at ∼2.3 and 10.4 μm.

The decrease in size and percentage of the smallest particles together with the appearance of populations of longer sizes after 20 h of sonication suggest that two process occur simultaneously: (1) A progressive particle-size reduction of the individual particles and (2) an agglomeration of some ultrasound-activated particles to form agglomerates larger than 5 μm. Delgado and Matiyevic [24] have reported that prolonged sonication of colloids yields agglomeration of particles.

Treatment II: Fig. 2II shows the particle-size distribution vs the percentage of particle volume of the untreated kaolinite and after different sonication times under the experimental conditions described for treatment II. Under these experimental conditions a minimum of 20 h of treatment is necessary to achieve notable results. For this reason we

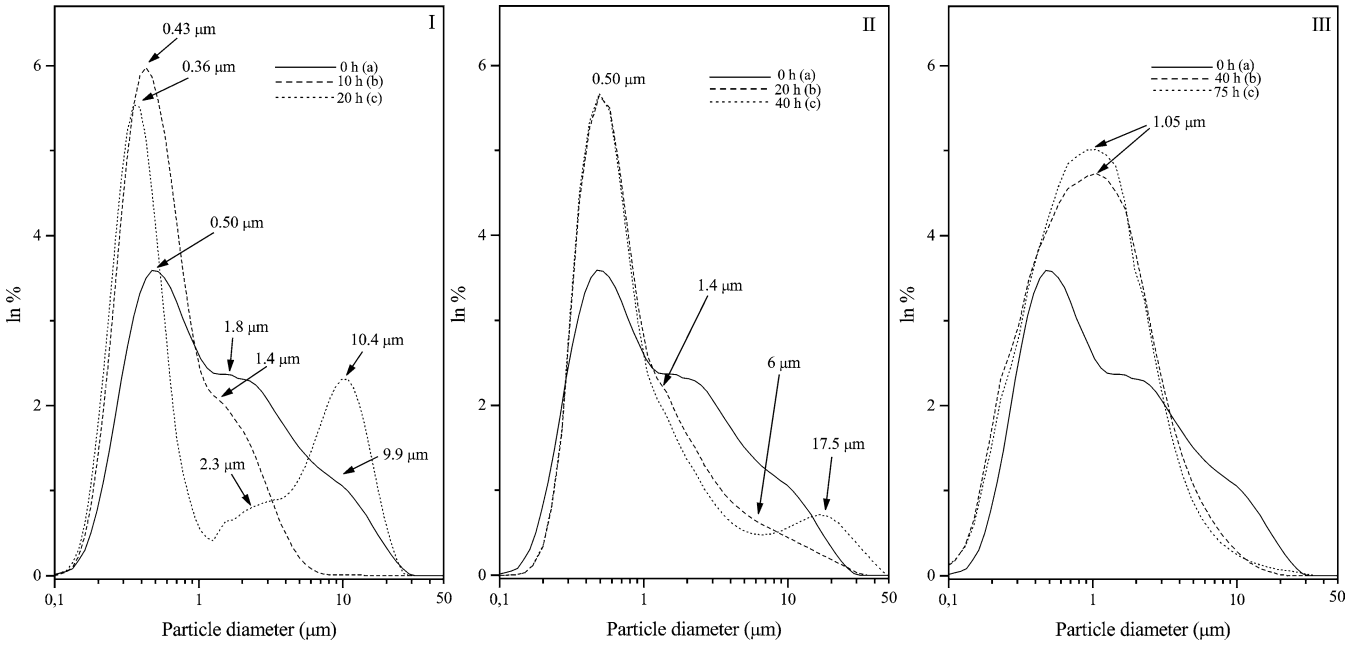

Fig. 2. Particle-size distribution versus percentage of particle volume determined by low-angle laser light scattering (LALLS) for kaolinite samples treated with ultrasound under different experimental conditions and at different sonication times. I: treatment I, $a = 0$ h, $b = 10$ h, $c = 20$ h; II: treatment II, $a = 0$ h, $b = 20$ h, $c = 40$ h; III: treatment III, $a = 0$ h, $b = 40$ h, $c = 75$ h.

present in this work the results obtained after 20 and 40 h of treatment.

After sonication periods of 20 h, the proportion of particles larger than 5 μm notably decreases, but they do not disappear completely, as occurred after 10 h in treatment I. In this case, the distribution curve (Fig. 2IIb) shows the presence of three populations with maxima at 0.50, ∼1.4, and ∼6 μm. The proportion of the smallest particles notably increases, as compared with the distribution curve of the starting kaolinite, but the maximum does not shift to lower values, as occurred in treatment I. Simultaneously, the proportion of the 1.8- and 9.9-μm populations, observed in the distribution curve of the starting kaolinite, notably decreases and the maxima appear as shoulders at ∼1.4 and ∼6 μm, respectively. After sonication periods of 40 h (Fig. 2IIc), the distribution curve shows that the 0.5-μm maximum remains almost unchanged, whereas the 1.4- and 6-μm maxima slightly decrease and a new group of particles appears with maximum volume percentage at 17.5 μm.

The results described above suggest that the ultrasonic power supplied under the experimental conditions of treatment II is insufficient to obtain kaolinite particles with sizes smaller than 0.50 μm (Fig. 2II). Nevertheless, at the longest sonication time (40 h), particles become agglomerated, as shown by the presence of a population with sizes higher than 10 μm in the particle-size distribution curve (Fig. 2IIc). Agglomeration is already observed for the sample sonicated under the conditions of treatment I after only 20 h.

Treatment III: Fig. 2III shows the particle-size distribution vs the percentage of particle volume of the untreated kaolinite and after different sonication times under the experimental conditions described for treatment III. Under these conditions a minimum of 40 h of treatment is necessary to achieve notable results. For this reason we present in this work the results obtained after 40 and 75 h of treatment.

After sonication periods of 40 h, the distribution curve shows that the percentage of particles with size higher than 5 μm notably decreases, whereas the proportion of the 1.8-μm particles increases considerably. In this case, the distribution curve (Fig. 2IIIb) shows only a band with a maximum at 1.05 μm, which cover the initial populations, observed in the untreated kaolinite, with maxima at 0.50 and ∼1.8 μm. The distribution curve obtained with longer sonication times (75 h, Fig. 2IIIc) does not show significant modifications. In this case, after 75 h of treatment an increase of the maximum volume percentage of the monomodal distribution is observed, together with a slight decrease of the proportion of particles with size greater than 3 μm.

These data show that the increase of the amount of the sample subjected to ultrasound in treatment III results in a decrease of the ultrasound energy per mass unit. Thus, although the resulting energy permits a particle-size reduction of the 9.9-μm population, the power supplied is apparently insufficient to reduce, to a great extent, the size of the 1.8-μm particles in up to 75 h treatment (Fig. 2IIIc). The increase of this latter population and the maintenance of that with a maximum at 0.50 μm give rise to the observed broad monomodal distribution, which covers a wide range of sizes (between 0.1 and 17 μm).

Fig. 3 shows the variation of specific surface area (SSA) for kaolinite, obtained with different treatments, as a function of sonication time in the different treatments. The obtained values of ssa are presented in Table 1. The variation

in ssa with treatment I is shown in Fig. 3I. This figure clearly reveals that sonication produces a remarkable increase in the SSA with the treatment time. The increase of the SSA is continuous and no evidence of decrease due to the formation of hard aggregates is observed even after 20 h of treatment. When the experiments are carried at under the experimental conditions of treatment I, SSA increases from 8.5 $m^2\,g^{-1}$ to 35.2 $m^2\,g^{-1}$ after 10 h of treatment. When the sonication time increases beyond 10 h, the SSA also increases, reaching 83 $m^2\,g^{-1}$ at 20 h. Thus, the surface area increases 10 times after 20 h of treatment.

When the ultrasonic processor used is less energetic (treatment II, Fig. 3II), the sonication also produces a remarkable increase in the SSA of the kaolinite; nevertheless longer treatments are necessary to achieve results similar to those observed with treatment I. Thus, the initial value of the original kaolinite (8.5 $m^2\,g^{-1}$) increases to 45 $m^2\,g^{-1}$ after 20 h of sonication. For sonication times of 40 h, the SSA increases to 67 $m^2 g^{-1}$.

The increase of the SSA in treatment III is shown in Fig. 3III. In 40 h of sonication treatment the SSA increases from 8.50 to 14.54 $m^2\,g^{-1}$. The SSA continues to increase with the time of treatment and at 75 h the SSA is 22.29 $m^2\,g^{-1}$. It is interesting to note that the increase in SSA with treatment III is notably slower than that obtained for treatments I and II. These data reveal that the effect of the sonication treatment is strongly influenced by the amount of sample (kaolinite + water).

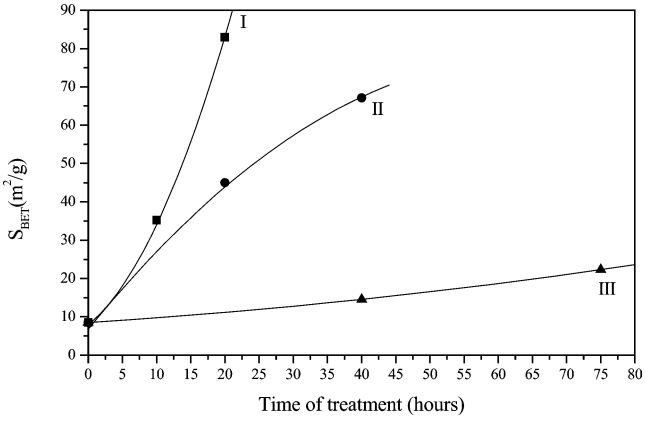

Fig. 3. Evolution of specific surface area under different experimental conditions. I: treatment I; II: treatment II; III: treatment III.

The results obtained with the different sonication treatments are notably different from those previously obtained [11] in the grinding of this kaolinite. Sánchez-Soto et al. observed that the SSA decreased after 20 min of grinding because the kaolinite particles became agglomerated. In this case, when the SSA is enhanced with an ultrasound treatment this increase is continuous with the time of treatment, reaching SSA values never obtained with this kaolinite. Possibly the different experimental conditions prevent the formation of hard aggregates.

Table 1 includes the values of the ESD calculated from the SSA values of Fig. 3. For the untreated kaolinite the ESD has a value of 266 nm. After 10 h of treatment I the kaolinite has an ESD of 64.3 nm. The ESD decreases to 27.29 nm after 20 h of treatment. The decrease of ESD obtained under the experimental conditions of treatment II are lower. The ESD values of the kaolinite decreases to 50.35 nm at 20 h and to 33.74 nm after 40 h. When the amount of the sample used in the treatment is higher (treatment III) the decrease of ESD is even lower. Thus, at 40 h of treatment the ESD value descends to 155.7 nm and decreases to 66.6 nm after 75 h.

The reduction in the particle size and the associated morphological changes that occurred during sonication of the standard kaolinite were clearly evident in the scanning electron micrographs (Figs. 1 and 4). Fig. 4a shows a SEM micrograph of the sample obtained by treating the original kaolinite with ultrasound for 10 h under the experimental conditions described for treatment I. After 10 h of sonication, the original stacking layers and kaolinite booklets were delaminated, and the particle size of the lamellar starting material was reduced. SEM micrographs show that these effects are also obtained with treatment II. Nevertheless, the slightly greater length of most of the particles observed after 40 h of treatment II (Fig. 4b) compared to that observed after 10 h of treatment I reveals that, even using longer times of treatment, the particle-size reduction obtained with treatment II is not so significant as that obtained with treatment I. This fact was already observed in the particle-size distribution curves obtained by LALLS.

The reduction in the particle size was also observed in TEM micrographs. The sample obtained after a sonication

Table 1
Specific surface areas, equivalent spherical diameters, and crystalline data of the starting kaolinite and of treated kaolinites

Sample	T (h)	SSA ($m^2\,g^{-1}$)	ESD (nm)	CS_{002}	CS_{060}	HI	R_2	D (131 to $1\bar{3}1$)
KGa-1[a]	0	8.50	266	424	261	1.19	0.99	0.86
Treatment I	10	35.20	64.3	368	231	0.33	0.88	0.84
Treatment I	20	82.95	27.29	270	202	0.21	0.71	0.72
Treatment II	20	44.97	50.35	353	248	0.60	0.95	0.80
Treatment II	40	67.10	33.74	351	229	0.53	0.94	0.78
Treatment III	40	14.54	155.7	377	242	0.61	0.96	0.82
Treatment III	75	22.29	66.6	355	241	0.54	0.94	0.78

[a] Starting kaolinite. T = Time of treatment in hours; SSA = specific surface area; ESD = equivalent spherical diameter; CS_{002} and CS_{060} = apparent coherent scattering thickness measured using the Scherrer formula on 002 and 060 reflection; HI = index of Hinckley [20]; R_2 = index of Lièrtard [21]; D = distance between 1 3 1 and $1\bar{3}1$.

period of 20 h under the experimental condition of treatment I (Fig. 5b) consists of thin plates that do not present a regular morphology due to the impact with other particles and to microjet and shock-wave impacts on the surface during the sonication treatment. The smallest particles exhibit sizes inferior to that observed in the untreated kaolinite (Fig. 5a).

It is interesting to remark the different results obtained from the different treatments. The distribution curves obtained after treatment I indicate that the power supplied was able to reduce the size of the particles to values lower than 0.5 μm (Fig. 2I). In contrast, treatment II can only reduce the size of the particles larger than 1 μm, as indicated by the distribution curves obtained after this treatment (Fig. 2II). The power supplied in this treatment is not able to reduce the size of the 0.5-μm particles. On the other hand, when the amount of kaolinite and water increases, as occurred in treatment III, the resulting energy per gram of kaolinite is notably reduced because the ultrasonic energy is distributed through the whole of the dispersion. Under these conditions, the effects of the ultrasound on the particle size are also reduced. Thus, the power supplied in treatment III can reduce the size of the particles larger than 5 μm, but is insufficient to reduce the size of the 1.8-μm population (Fig. 2III). These results indicate that the particle sizes of the treated kaolinite strongly depend on the power supplied with the ultrasonic processor but also on the amount of sample used in the treatment. It may be possible to obtain particles with specific sizes through the control of the power supplied. Nevertheless, this deserves a more detailed investigation.

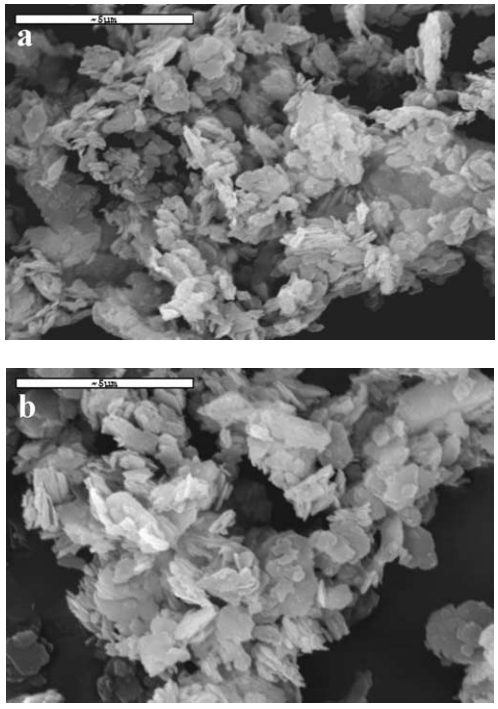

Fig. 4. Selected scanning electron micrograph of kaolinite after 10 h of treatment I (a) and 40 h of treatment II (b).

3.2. XRD study

We must keep in mind that the different methods used to measure particle sizes of very different physical magnitudes, i.e., scattering of light (LALLS) and adsorption of nitrogen at liquid-nitrogen temperature (ESD), assume that particles are spherical. For this reason, considering that kaolinite is a lamellar silicate, it is of interest to obtain information on the dimensions in different crystallographic directions. Methods based on the broadening of the X-ray diffraction peaks average diffraction effects from a large number of individual kaolinite crystallites and give information on dimensions in a particular crystallographic direction. Also these sizes are related to microdomains of coherent scattering and not to agglomerates.

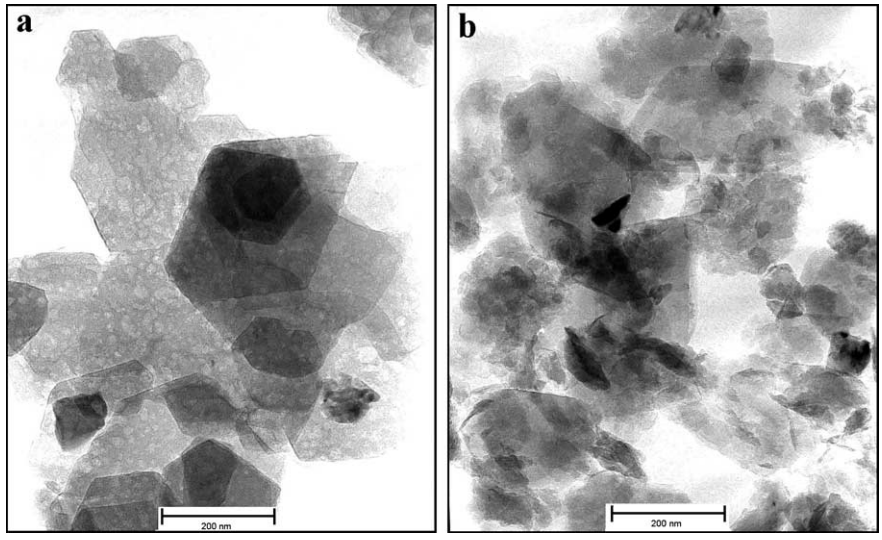

Fig. 5. Selected transmission electron micrograph of untreated kaolinite (a) and kaolin after 20 h of treatment I (b).

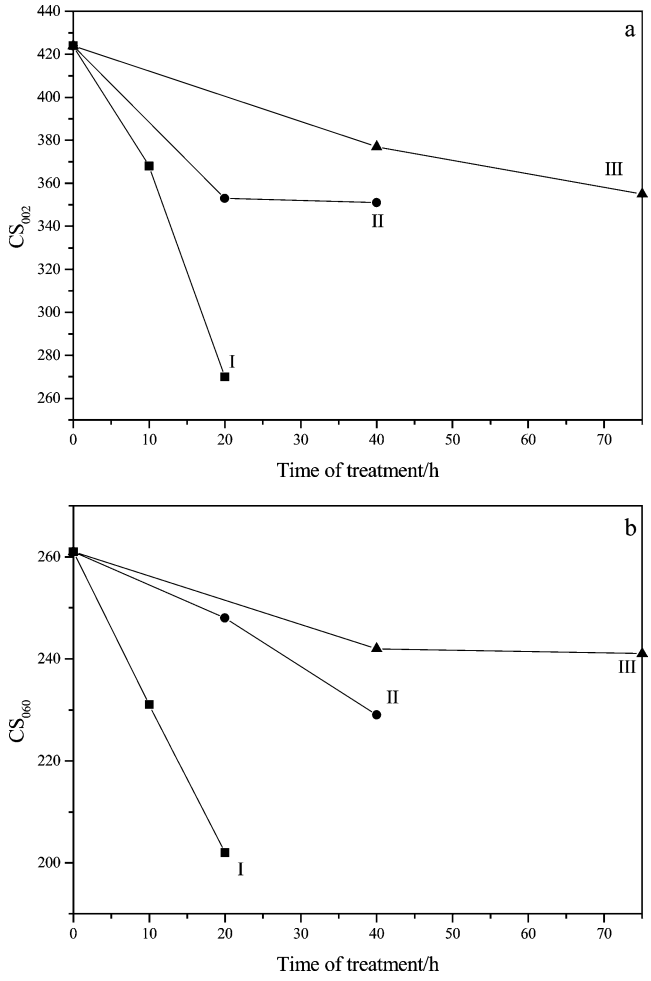

Fig. 6. Evolution of the apparent coherent scattering thickness of the kaolinite crystals along the c^* axis (a) and along the b axis (b). I: treatment I; II: treatment II; III: treatment III.

Fig. 6a includes the crystallite size of untreated kaolinite (KGa-1) and sonicated samples as calculated by the Scherrer broadening method using the 0 0 2 reflection. This latter is a basal reflection and may be used for direct estimation of the particle thickness. The value of the coherent diffraction thickness along the c^* axis of the kaolinite subjected to ultrasound under the experimental conditions of treatment I decreases from 424 to 368 Å after 10 h of sonication and to 270 Å after 20 h (Table 1, Fig. 6aI). The rate of decrease of the thickness of kaolinite is lower if the treatment is carried out under the conditions of treatments II and III. Thus, in treatment II, the coherent diffraction thickness along the c^* axis decreases from 424 to 353 Å after 20 h and to 351 Å after 40 h of sonication (Fig. 6aII). Under the experimental conditions of treatment III, longer time of treatment are necessary to achieve similar results to that observed in treatment II (Fig. 6aIII, Table 1).

The ultrasound treatment also causes the progressive broadening of the 0 6 0 reflection, which indicates that the dimension of kaolinite crystals along their b axis also decreases with the time of ultrasound treatment (Table 1, Fig. 6b) due to the transverse breakage of the kaolinite flakes. As expected, the highest rate of decrease of the particle size along the b axis is obtained with the most energetic treatment (treatment I). Under this experimental condition, the coherent scattering thickness along the b axis decreases from 261 to 202 Å in 20 h of treatment. Fig. 6b shows that the rates of decrease of the particle size along the b axis obtained with treatments II and III are notably lower.

Fig. 7Ia shows the powder XRD patterns of the starting Georgia kaolinite between 20 and 40° 2θ. The reflections $0\,2\,l$, $1\,1\,l$ and $2\,0\,l$, $1\,2\,l$ are narrow and intense, indicating that this kaolinite is well-crystallized. Important modifications of the $0\,2\,l$, $1\,1\,l$ reflections are observed with the time of treatment. These reflections are very sensitive to the abundance of translation defects consisting in random and specific interlayer displacements of type $-a/3 + b/3$ [25]. We have used the HI [20] to evaluate the modifications in this zone of diagrams (20°–22° 2θ) and to assigning a numerical value to the degree of structural disorder (Table 1, Fig. 8a).

In treatment I, the decrease of the Hinckley index from 1.19 to 0.33 indicates that a great increase in translation defects takes place at 10 h of treatment. On the other hand, between 10 and 20 h of sonication the increase in translation defect is sensibly smaller (Table 1, Fig. 8a). Although the greatest decreases of *HI* are obtained under the experimental conditions of treatment I, the power supplied in treatments II and III also causes remarkable decreases in *HI* (Table 1, Fig. 8a).

Minor modifications are caused in the $2\,0\,l$, $1\,3\,l$ reflections. This zone of diagrams (35°–40° 2θ) is also affected by random displacement [22]. Plançon and Zacharie [25] showed that increasing the small displacements (random displacements) between adjacent layers is the principal effect of reducing the 1 3 1 reflection relative to the $1\,\bar{3}\,1$ reflection. We have used the R_2 index [21,22] to measure the modifications in this zone of the diffractograms. Variations of the R_2 index with sonication time are shown in Fig. 8b. In contrast to the observed variations of *HI*, which are very sensitive to the effects of the different sonication treatments evaluated here, the lower decreases of the R_2 index after treatments II and III indicate that under these experimental conditions the power supplied increases considerably the proportion of specific interlayer displacement of type $-a/3+b/3$, as indicated by the decreases of *HI*, but it is insufficient to generate a great increase in the proportion of random displacements between layers.

A slight narrowing of the distance between 1 3 1 and $1\,\bar{3}\,1$ reflections (Table 1) is related to a minor difference between γ and 90°. It leads to the formation of layers having vacant octahedral *C*-sites (dickite-like layers) [25]. The distance of these reflections is reported in Table 1.

The XRD patterns of the treated samples indicate that the structural changes induced by the ultrasound treatment are time-dependent. Thus, after 10 h of treatment I, the ultrasound energy caused a great increase in the abundance

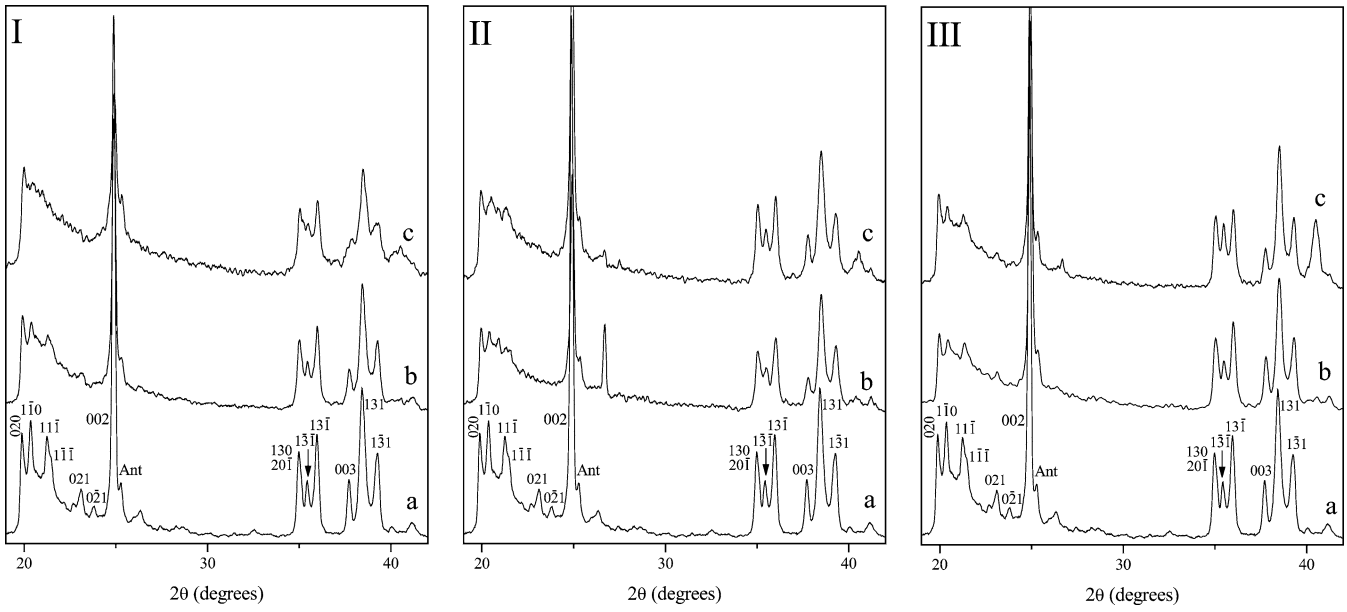

Fig. 7. XRD patterns of the kaolinite samples treated with ultrasound under different experimental conditions and at different sonication times. I: treatment I, $a = 0$ h, $b = 10$ h, $c = 20$ h; II: treatment II, $a = 0$ h, $b = 20$ h, $c = 40$ h; III: treatment III, $a = 0$ h, $b = 40$ h, $c = 75$ h.

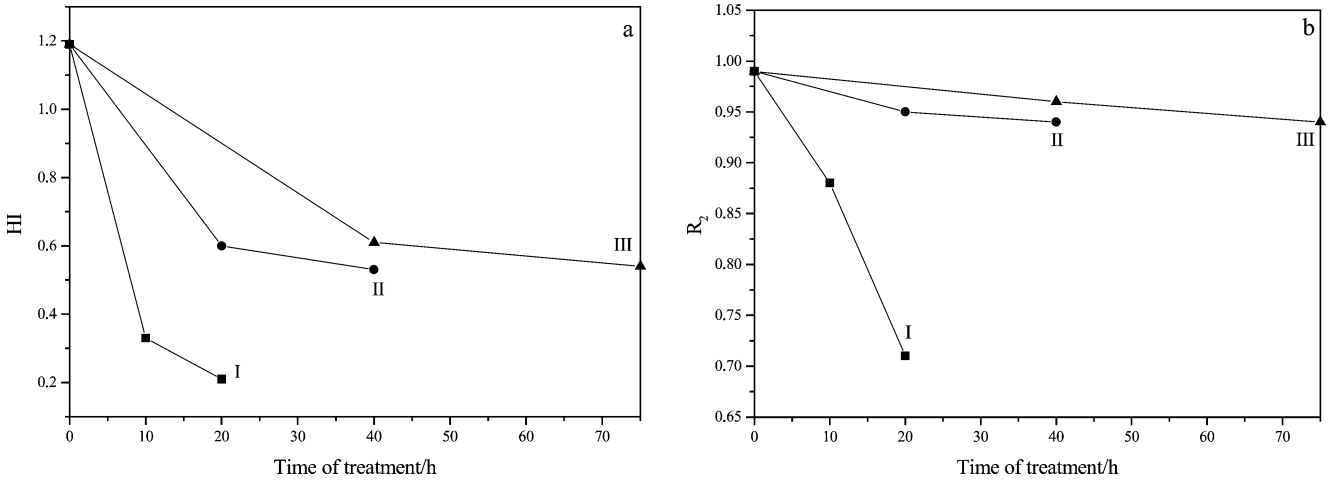

Fig. 8. Evolution of the *IH* (a) and R_2 (b) indexes. I: treatment I; II: treatment II; III: treatment III.

of translation defects consisting of displacements of type $-a/3 + b/3$ and random translations, as shown by the great decrease of the *HI* and R_2 indexes. In addition, a decrease of the thickness of the kaolinite plates and a minor decrease of the dimensions of the particles along their *b* axes are also observed. In the interval between 10 and 20 h, the ultrasound energy of treatment I caused a minor decrease in the *HI*, but a greater decrease of the R_2 index, which indicates that the increase in the proportion of random translations continues. In this time of treatment, a greater decrease of the CS_{002} parameter, compared to that obtained in the first 10 h of treatment I, is observed. Moreover, the variation in the CS_{060} shows a similar cross breakage of the kaolinite particles compared to that obtained in the first 10 h of treatment. However, in spite of the formation of translation defects and the reductions of particle size, the kaolinite still remains crystalline, contrary to what was observed previously in the grinding treatments, where the total degradation of the kaolinite structure, probably related to the rupture of the octahedral and tetrahedral layers, is reported for long grinding times [11]. Perhaps the dilution by water protects the kaolinite from amorphization during the ultrasound treatment.

3.3. FTIR study

The OH stretching region of the FTIR spectra of the untreated kaolinite (KGa-1) is shown in Fig. 9Ia. This spectrum shows the expected four bands in the νOH region at 3694, 3668, 3651, and 3619.5 cm^{-1} (ν_1, ν_2, ν_3, and ν_4, respectively). These bands are assigned as follows: The

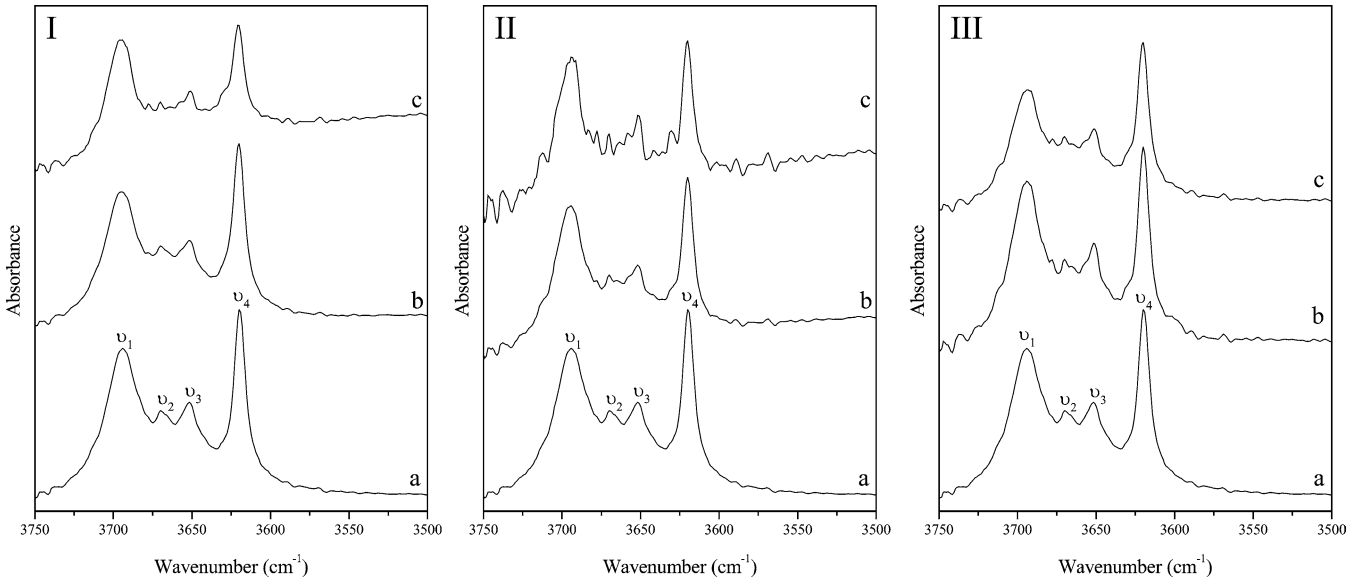

Fig. 9. OH stretching region of the FTIR spectra of the kaolinite samples treated with ultrasound under different experimental conditions and at different sonication times. I: treatment I, $a = 0$ h, $b = 10$ h, $c = 20$ h; II: treatment II, $a = 0$ h, $b = 20$ h, $c = 40$ h; III: treatment III, $a = 0$ h, $b = 40$ h, $c = 75$ h.

3619.5 cm^{-1} band (band ν_4) is caused by the vibrational mode of the inner hydroxyl group, which is situated in the plane shared between the octahedral and the tetrahedral sheets in the same layer [26]. The other three bands are related to the vibrations of the three inner-surface hydroxyls. These inner-surface hydroxyl groups couple to give a strong in-phase symmetric stretch at 3694 cm^{-1} (band ν_1) with a transition moment close to c^* and two weak out-of-phase vibrations at 3668 and 3651 cm^{-1} (bands ν_2 and ν_3, respectively) with transition moments in the (0 0 1) plane [13,27].

The spectrum of the untreated kaolinite shows the following bands in the 1200–850 cm^{-1} region (Fig. 10Ia): 1117, 1093, 1030, 1008, 939, and 913 cm^{-1}. Bands at 1117 and 1093 cm^{-1} (bands SiO_1 and SiO_2, respectively) are related to Si–O out-of-plane vibrations and bands at 1030 and 1008 cm^{-1} (bands SiO_3 and SiO_4, respectively) are Si–O in-plane vibrations [14,15]. Bands centered at 938.5 and 913 cm^{-1} (bands δ_1 and δ_2, respectively) have been assigned to the inner surface and inner hydroxyls deformation modes, respectively [27].

As the time of treatment increases a series of changes take place in the OH stretching region (Fig. 9): (1) increases of noise/signal ratio and (2) changes in the intensity of νOH bands.

The increase of noise cannot be observed in the FTIR spectra obtained after 10 h of treatment I because all the presented spectra are smoothed in order to facilitate the comparison of the positions and areas of νOH bands. Nevertheless, it can be clearly observed above 20 h in all cases (Fig. 9).

The hydroxyl group is able to reorient in response to changes in the local structural environment. For this reason we can assume that its orientation corresponds to a potential energy minimum. The increase of the noise can be explained by changes in the OH orientation to more energetic positions caused by the absorption of the ultrasonic energy. This increase is fundamentally dependent on the time of treatment. In all cases, signal/noise ratio decreases with time.

Another effect of the ultrasound in the spectra of the kaolinite is the decrease in the intensity of the OH stretching (ν_{1-4}) and deformation bands (δ_{1-2}) (Figs. 9 and 10). This effect was traditionally related to the disorder in the stacking of the layers [27,28], but these bands are not sensitive to specific translational faults of type $-a/3 + b/3$ because they do not produce appreciable modifications in the environment of the OH inner surface hydroxyls. Translations by $-a/3 + b/3$ leave the OH groups in a practically identical position relatively to the basal oxygens of the adjacent layer [29]. Nevertheless, the decrease in absorbance of the inner hydroxyl band (ν_4) (Fig. 9I), which is not affected by the translational defects due to its orientation, indicates that prototrophy occurs [14,15], and it affects the intensity of the OH bands. Perhaps this process takes place on the new surface generated in the delamination.

On the other hand, according to Farmer and Russell [13], delamination can be examined from the intensity and position of the Si–O vibrational bands, which gives a dipole oscillation perpendicular to the plates. Yariv [14,15] related the increase of absorbance and a red-shift of the band at 1098 cm^{-1} (band SiO_2) to the delamination of kaolinite during the grinding with KBr. In our case, the behavior of the SiO_2 band is similar to that reported by Yariv [14,15]. This band is shifted to higher wavenumber after sonication treatment; e.g., after 20 h of treatment I this band is shifted from 1093 to 1100 cm^{-1} (Fig. 10I). Similar shifts can be observed in the FTIR spectra of the ultrasound-treated kaolinite under the experimental conditions of treatments II and III (Fig. 10II and 10III). Therefore, these results clearly

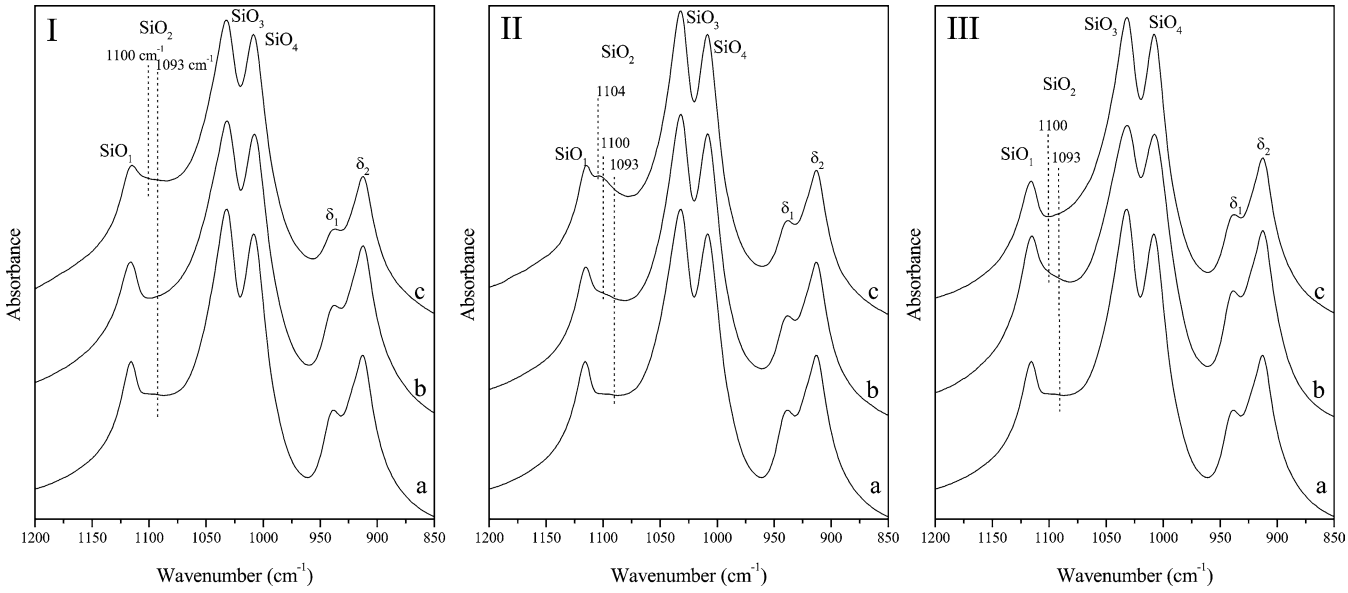

Fig. 10. The 850–1200 cm^{-1} region of the FTIR spectra of the kaolinite samples treated with ultrasound under different experimental conditions and at different sonication times. I: treatment I, $a = 0$ h, $b = 10$ h, $c = 20$ h; II: treatment II, $a = 0$ h, $b = 20$ h, $c = 40$ h; III: treatment III, $a = 0$ h, $b = 40$ h, $c = 75$ h.

indicate that delamination takes place during the sonication treatment.

On the other hand, Yariv [14,15] also observed that SiO_3 and SiO_4 bands were strongly affected by the formation of amorphous material during grinding. These bands, which are Si–O in-plane vibrations, give information about whether the tetrahedral sheet is more or less uniform. In our case, the sonication treatment does not modify either the intensity or the position of bands at SiO_3 and SiO_4 (Fig. 10); therefore we can conclude that the symmetry of the tetrahedral sheet is not affected by the ultrasound treatment.

4. Conclusions

Sonication of a well-ordered kaolinite produces not only an important delamination effect on the kaolinite sample but also a reduction of the other particle-size dimension. The particle-size reduction by ultrasound is a process controlled by different variables such as power of the ultrasonic processor, time of treatment, and amount of sample (kaolinite + water). As a consequence of this particle-size reduction the surface area increases sharply with sonication time. In contrast to what is observed in the grinding treatments, sonication does not cause the amorphization of kaolinite as observed by DRX and FTIR data. Perhaps the dilution by water protects the kaolinite from amorphization during the ultrasound treatment. Nevertheless, ultrasound treatments increase the structural disorder, which consist in increases in the proportion of specific translations $(-a/3 + b/3)$ between adjacent layers, in the first hours of treatment, followed by increases in the proportion of random translations.

References

[1] C.C. Harvey, H.H. Murray, Appl. Clay Sci. 11 (1997) 285.
[2] H.H. Murray, Appl. Clay Sci. 17 (2000) 207.
[3] C.S.F. Gomes, in: C.S.F. Gomes (Ed.), Argilas: Aplicaçoes na Industria, 2002, p. 338.
[4] W.M. Bundy, in: H.H. Murray, W. Bundy, C. Harvey (Eds.), Kaolin, Genesis and Utilization, Special Publication, vol. 1, The Clay Minerals Society, 1993.
[5] S.C. Lyons, in: Itagemeyer (Ed.), Clay, in: T.A.P.P.I. Monographs, vol. 30, 1966.
[6] E. Galán, P. Aparicio, I. González, A. Miras, Clay Miner. 33 (1998) 65.
[7] Th. De Putter, L. André, A. Bernard, Ch. Dupuis, J. Jedwab, D. Nicaise, A. Perruchot, Appl. Geochem. 17 (2002) 1313.
[8] A.E. Osmanlioglu, Waste Manage. 22 (2002) 481.
[9] G. Suraj, C.S.P. Iyer, S. Rugmini, M. Lalithambika, Appl. Clay Sci. 12 (1997) 111.
[10] G. Baudet, V. Perrotel, A. Seron, M. Stellatelli, Powder Technol. 105 (1999) 125.
[11] P.J. Sánchez-Soto, M.C. Jiménez de Haro, L.A. Pérez-Maqueda, I. Varona, J.L. Pérez-Rodríguez, J. Am. Ceram. Soc. 83 (7) (2000) 1649.
[12] F. González-García, M.T. Ruiz-Abrio, M. González-Rodríguez, Clay Miner. 26 (1991) 549.
[13] V.C. Farmer, J.D. Russell, Spectrochim. Acta 22 (1966) 389.
[14] S. Yariv, Clays Clay Miner. 23 (1975) 80.
[15] S. Yariv, Powder Technol. 12 (1975) 131.
[16] D. Peters, J. Mater. Chem. 6 (1996) 1605.
[17] J.A.G.L. Velho, C.S.F. Gomes, Appl. Clay Sci. 6 (1991) 155.
[18] L.A. Pérez-Maqueda, O.B. Caneo, J.P. Poyato, J.L. Pérez-Rodríguez, Phys. Chem. Miner. 28 (2001) 61.
[19] J.L. Pérez-Rodríguez, F. Carrera, J. Poyato, L.A. Pérez-Maqueda, Nanotechnology 13 (2002) 382.
[20] D. Hinckley, Clays Clay Miner. 11 (1963) 229.
[21] O. Lièтard, Contribution à l'étude des propiétés phisicochimiques, cristallographiques et morphologiques des kaolins, Ph. D. thesis, Nancy, France, 1977, p. 345.
[22] J.M. Cases, O. Lièтard, J. Yvon, J.F. Delon, Bull. Mineral. 105 (1982) 439.

[23] B.D. Cullity, in: M. Cohen (Ed.), Elements of X-Ray Diffraction, Addison–Wesley, Reading, MA, 1956, p. 514.
[24] A. Delgado, E. Matiyevic, Part. Part. Syst. Charact. 8 (1991) 120.
[25] A. Plançon, C. Zacharie, Clay Miner. 25 (1990) 249.
[26] R.L. Ledoux, J.L. White, Science 145 (1964) 47.
[27] V.C. Farmer, J.D. Russell, Spectrochim. Acta 20 (1964) 1149.
[28] G.W. Brindley, Kao Chich-Chgun, J.L. Harrison, M.L. Lipsicas, R. Raythata, Clays Clay Miner. 34 (1986) 239.
[29] J. Barrios, A. Plaçon, M.I. Cruz, C. Tchoubar, Clays Clay Miner. 25 (1977) 422.